Singular Value Decomposition of Munsell Color Samples: Principal Hue Components

T. Indow and A.K. Romney
Department of Cognitive Sciences, University of California, Irvine
Irvine CA 92612 (U.S.A.)
Corresponding author: (tindow@uci.edu)

ABSTRACT
From reflected light spectra of Munsell chips j under D65, two matrices, $\overline{\mathbf{P}}$ and $\overline{\mathbf{W}}$, are extracted that have the following properties. (1) Their combination reproduces the spectra of light. (2) $\overline{\mathbf{P}}$ defines a 3-D structure related to the Munsell solid. (3) $\overline{\mathbf{W}}$ defines, in the plane corresponding to H and C, a curve related to wavelength and Munsell hue circle. (4) These are related to the perceived principal hue components, R, Y, G, B, in Munsell chips j.

1. SINGULAR VALUE DECOMPOSITION (SVD)

It was shown in a previous article[1] that reflected light spectra $s_{j\mu}$ of Munsell chips under D65 is represented as the product of two matrices, $\overline{\mathbf{P}}(\overline{p}_{j\gamma})$ and $\overline{\mathbf{W}}(\overline{w}_{\mu\gamma})$ obtained by SVD and a rigid rotation.

$$\mathbf{S}=(s_{j\mu}) \approx \hat{\mathbf{S}}=(\hat{s}_{j\mu})=\overline{\mathbf{P}}\,\overline{\mathbf{W}}^{T} \quad (1)$$

j = 1, 2, ..., 370 (360 color chips (5H varying in V and C) plus 10 grays)
μ = 1, 2, ..., 231 (wavelength λ from 430-660 nm with a step of 1 nm)
$s_{j\mu}$ = $r_{j\mu}$ (spectral reflectance of chip j) × e_{μ} (relative spectral radiant power of D65) (2)
γ = 1, 2, 3 (orthogonal axes defined by SVD and a rigid rotation).

How closely $\hat{\mathbf{S}}$ reproduces the data **S** is shown in Fig.5 of another article[2]. The first column vector $\overline{\mathbf{P}}1$ of $\overline{\mathbf{P}}$ represents radiant intensity (Fig.1) whereas the second and third column vectors $\overline{\mathbf{P}}2$ and $\overline{\mathbf{P}}3$ define Hue H, Chroma C, and $(\overline{p}_{j2}, \overline{p}_{j3})$ of all intensity levels in a plane perpendicular to $\overline{\mathbf{P}}1$ (similar to Fig.2). The axes are defined so that $\overline{\mathbf{P}}2$ places 5R chips at the top of the diagram.

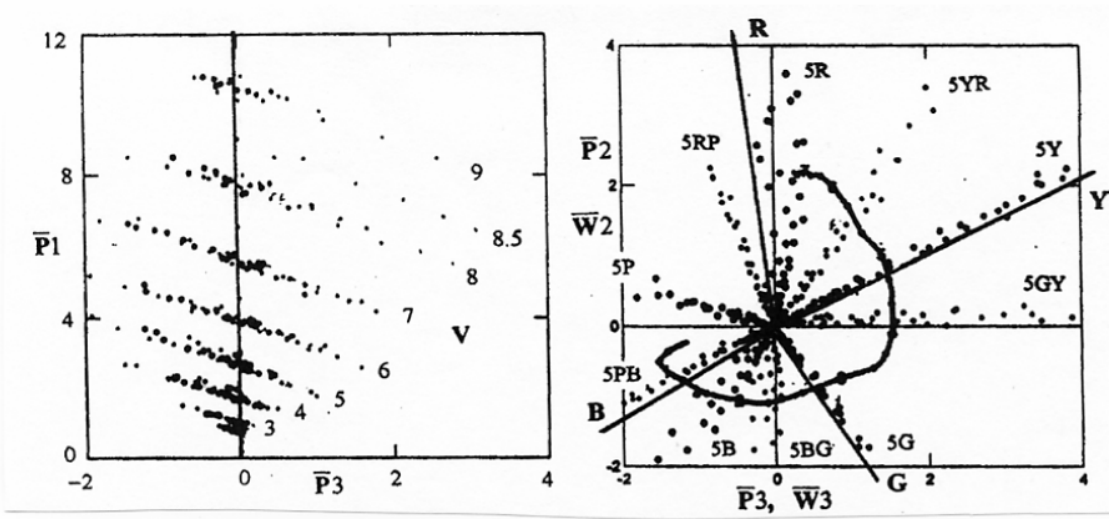

Fig. 1: View of $\overline{\mathbf{P}}$ from the direction of $\overline{\mathbf{P}}2$

Fig.2: (H,C) plane tilted 38° to $\overline{\mathbf{P}}1$, the spectral curve $\overline{\mathbf{W}}$ and principal hue axes superimposed.

In Fig.1, gray chips are represented on the vertical line ($\overline{\mathbf{P}}3 = 0$) and color chips of same Value V form a thin layer of dots. These layers are tilted with regard to $\overline{\mathbf{P}}1$ but almost parallel with an angle of 38^{O}. The tilt of layers of constant V is due to the fact that Munsell V is defined in luminous intensity Y. We tried SVD analysis with defined as ($r_{j\mu} \times e_{\mu} \times \overline{y}_{\mu}$) instead of (2). Then, all layers became almost perpendicular to $\overline{\mathbf{P}}1$, but the structure of (H, C) configuration in Fig.2 was severely distorted in the P-region. Hence, we accept the results from $s_{j\mu} = (r_{j\mu} \times e_{\mu})$ as such.

The first column vector $\overline{w}_{\mu 1}$ of $\overline{\mathbf{W}}$ represents the radiant component in spectrum λ (= μ) (Fig. 3 in the article[1]). By the second and third vectors, the spectral curve was first defined on the ($\overline{\mathbf{P}}2$, $\overline{\mathbf{P}}3$) plane perpendicular to $\overline{\mathbf{P}}1$ (430nm on the lower left and 660nm on the upper middle). The unit of ($\overline{w}_{\mu 2}$, $\overline{w}_{\mu 3}$) was adjusted so that we could see the spectral curve and the configuration ($\overline{p}_{j2}$, $\overline{p}_{j3}$) in the same plot. Then, all the plotted results were vertically projected along $\overline{\mathbf{P}}1$ to a plane tilted with 38^{O}. Fig.2 was obtained in this way. From now on, $\overline{\mathbf{P}}2$ and $\overline{\mathbf{P}}3$ imply the coordinate axes in this plane. Notice that the achromatic origin of the configuration is preserved and in Fig.2 the radial distance ρ_j from the origin to a point j represents Chroma C_j of this Munsell chip.

2. PRINCIPAL HUE COMPONENTS

Based on human assessments of the degree of principal hue α in Munsell colors, Indow[3] defined, in the Munsell (H, C) plane, principal hue vectors $\{\mathbf{f}\alpha\}$ that are independent of V (α = 4 (R,Y,G,B), or 5 (R,Y,G,B,P) as in the Munsell Hue notation). It was found that $\mathbf{f}_P$ is redundant. Four $\mathbf{f}$'s are introduced in the (H, C) plane of Fig.2. This plane is also independent of V. Symbols to be used in the following discussion are listed below.

$\mathbf{f}_{\alpha}$ principal hue vectors in (H,C) plane, α = R, Y, G, B

$\overline{\mathbf{P}}2$, $\overline{\mathbf{P}}3$ orthogonal coordinate axes in Fig.2, tilted to $\overline{\mathbf{P}}1$ with an angle of 38^{O}

$\xi_{\alpha}(\lambda)$ coordinates (≥0) on $\mathbf{f}_{\alpha}$ of λ on the spectral curve in Fig.2

R_j, Y_j, G_j, B_j coordinates (≥0) of ($\overline{p}_{j2}$, $\overline{p}_{j3}$) on $\mathbf{f}_{\alpha}$ in Fig.2, α = R, Y, G, B

$\rho_j = \left(\overline{p}_{2j}^2 + \overline{p}_{3j}^2 \right)^{0.5}$ distance from the achromatic origin to point j in Fig.2 to represent C_j

$\xi_{\alpha 0}(H)$ coordinates (≥0) on $\mathbf{f}_{\alpha}$ of the Hue circle H, defined from the spectral curve in Fig.2

$\xi_{\alpha j} = \xi_{\alpha 0}(H) \times \rho_j$ principal hue components in chip j, α = R, Y, G, B (3)

$\overline{R}_j, \overline{Y}_j, \overline{G}_j, \overline{B}_j$ human assessments of principal hue components in chip j

$\hat{R}_j, \hat{Y}_j, \hat{G}_j, \hat{B}_j$ principal hue components in chip j predicted from R_j etc. or ξ_{Rj} etc.

$$\hat{R}_j = \alpha_R R_j^{\beta R} \quad etc. \tag{4}$$

or

$$\hat{R}_j = \alpha_R \xi_{R_j}^{\beta R} \quad etc. \tag{5}$$

$\mathrm{RMS} = \left(N^{-1} \sum (\overline{R}_j - \hat{R}_j)^2 \right)^{0.5}$ *etc.* root-mean-square of discrepancies, N = the number of cases in which $\overline{R}_j > 0$ and $\hat{R}_j > 0$

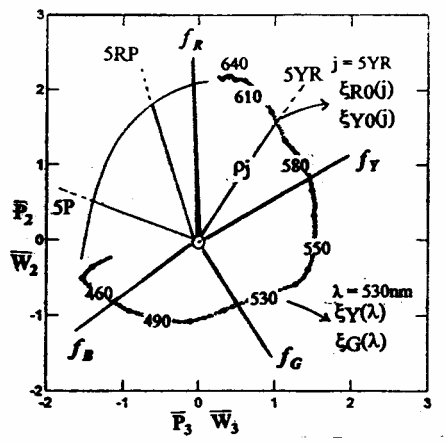

Fig.3: Spectral curve and principal hue vectors in Fig.2.

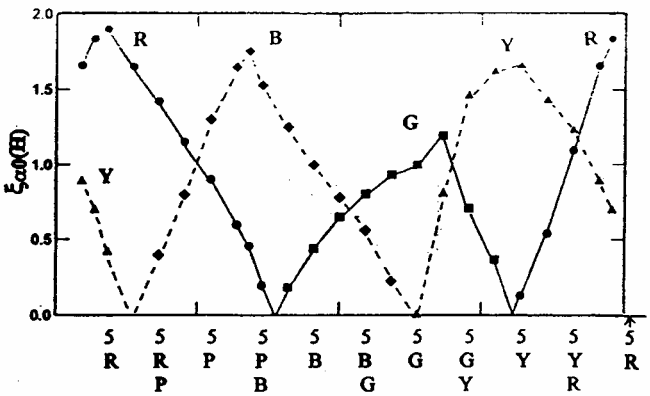

Fig.4: $\xi_{\alpha 0}(H)$ on the Hue circle H defined from the spectral curve in Fig.2

Values of $\xi_\alpha(\lambda)$ and R_j, Y_j, G_j, B_j can be directly defined in Fig.2. For j and λ in the quadrant between $\mathbf{f}_\alpha$ and $\mathbf{f}_\beta$, these are positive (Fig.3). The curves $\xi_{\alpha 0}(H)$ are shown in Fig.4. These are coordinates of the intersection of spectral curve (the numbers represent λ in nm) and the central direction in each series of H-points in Fig.2 (Fig.3). To define $\xi_{\alpha 0}$(5RP) *etc*., extrapolation over the extra-spectrum region was necessary. The extrapolation was carried out both in Fig.2 and in the $\xi_\alpha(\lambda)$ curves plotted against λ. The extrapolation was easier in the latter than in the former.

The main purpose of this presentation is to relate the results of SVD to principal hue components assessed by human observers, $\overline{R}_j, \overline{Y}_j, \overline{G}_j, \overline{B}_j$, (Indow[3,4,5]). As in Indow[3], the relationship is assumed to be power functions. As the independent variable, we can think of either R_j, *etc*., or ξ_{Rj} *etc*. defined in Eq.(3), Eqs.(4) or (5). Eq.(4) does not make use of the information in $\overline{\mathbf{W}}$. Eq.(1) analyzes the information in $s_{j\mu}$, the reflected light from Munsell chip j under D65, into two parts, $(\overline{w}_{\mu 2}, \overline{w}_{\mu 3})$ and $(\overline{p}_{j2}, \overline{p}_{j3})$, in addition to $\overline{\mathbf{P}}1$ and $\overline{\mathbf{W}}1$. The former is independent of V_j and C_j and the latter modifies the former in accordance with V_j and C_j, Eq.(3). Both Eqs.(4) and (5) were fitted and gave similar results. If we take further steps to discuss about cone activities[6] or activities in LGN caused by $s_{j\mu}$, Eq.(5) will be more useful.

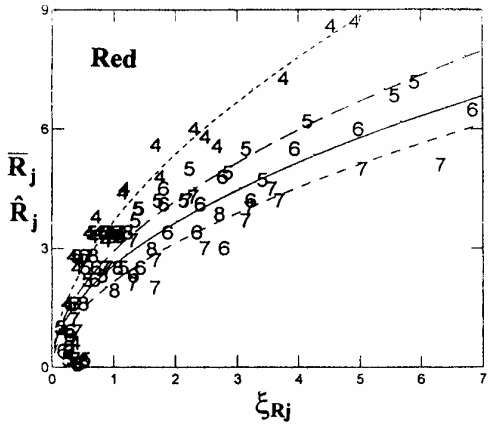

V	α_R	β_R	RMS	(RMS)
4	3.68	0.54	0.58	(0.88)
5	2.92	0.52	0.68	(0.85)
6	2.57	0.51	0.68	(0.60)
7 8	2.16	0.54	0.69	(0.49)

Fig.5. $\overline{R}_j$, $\hat{R}_j$ *vs*. ξ_{Rj}, plotted numbers represent V_j.

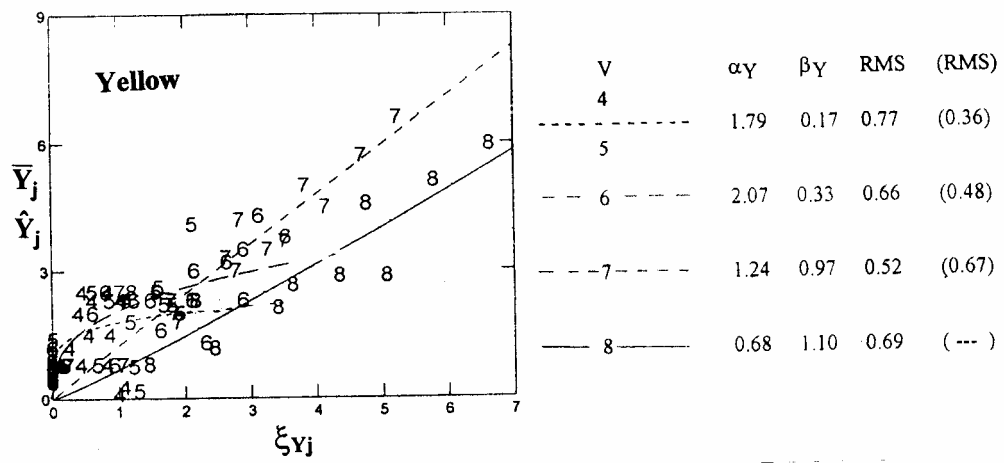

Fig. 6. $\overline{Y}_j, \hat{Y}_j$ *vs.* ξ_{Yj}, plotted numbers represent V_j

Two examples are shown in Figs.5 and 6. The numbers plotted represent V_j. Parameter values and RMS are given on the right side. The root-mean-square of scatter of points, RMS, is given with the unit of $\overline{R}_j$ *etc*. and hence it is comparable with RMS in Indow[3] in which $\overline{R}_j$ *etc*. are plotted against Cj. The value in the parentheses is RMS in this fit. Plots of $\overline{G}_j, \hat{G}_j$ *vs.* ξ_{Gj} or Gj and $\overline{B}_j, \hat{B}_j$ *vs.* ξ_{Bj} or B_j exhibit patterns more or less similar to Fig. 5. On the other hand, curves in plots, $\overline{Y}_j, \hat{Y}_j$ *vs.* ξ_{Yj} and $\overline{Y}_j, \hat{Y}_j$ *vs.* Y_j , exhibit a very different pattern (Fig.6). For $V_j < 7$, points clutter in the left corner and the fitted curves not necessarily represent their pattern. For $V_j = 7$ the curve is almost linear, and for $V_j > 7$ they are accelerated. This pattern for yellow was not observed in the plot of $\overline{Y}_j$ *vs.* C_j in Indow[3]. Except in Fig.5, values of RMS in the present plots tend to be of the same order of magnitude or larger than those in Indow[3].

SVD analysis of **S** gives $\overline{\mathbf{P}}$ and $\overline{\mathbf{W}}$ that not only reproduce **S** but also give two kinds of information, one yields the 3-D structure related to the Munsell solid and the other makes explicit the effect of wavelength λ, Eq (1). Their combination $\xi_{\alpha j}$ represents the perceived amount of principal hue components α in Munsell chip j under D65.

References

1. A.K. Romney and T. Indow, "A model for the simultaneous analysis of reflectance spectra and basis factors of Munsell color samples under D65 illumination in three-dimensional Euclidean space," Proceedings of National Academy of Sciences of USA, **99**, 11543-11546 (2002).
2. A.K. Romney and T. Indow, "Munsell reflectance spectra represented in three-dimensional Euclidean space," Color Research and Application, **28**, 182-196 (2003).
3. T. Indow, "Predictions based on Munsell notation, II. Principal hue components," Color Research and Application, **24**, 19-32 (1999).
4. T. Indow, "Color difference predicted by color component differences," Color Research and Application, **27**, 425-429 (2002).
5. T. Indow, "Psychologically unique hues in aperture and surface colors", Die Farbe, **34**, 253-260 (1987).
6. A.K. Romney and T. Indow, "Estimating physical reflectance spectra from human color-matching experiments," Proceedings of National Academy of Sciences of USA, **99**, 14607-14610 (2002).